ELSEVIER

Tectonophysics 267 (1996) 275–290

TECTONOPHYSICS

Orientation of nucleating faults in anisotropic media: insights from three-dimensional deformation experiments

S. Hanmer [a,b,*], D. Corrigan [a], A. Ganas [a]

[a] Ottawa-Carleton Geoscience Centre, Department of Earth Sciences, Carleton University, Ottawa, K1S 5B6, Canada
[b] Geological Survey of Canada, 601 Booth St, Ottawa, K1A 0E8, Canada

Received 30 May 1995; accepted 14 May 1996

Abstract

Physical experiments have been undertaken to investigate the influence of planar rheological anisotropy on the orientation of fault structures in three-dimensional flow associated with layer-normal shortening. The experimental results indicate that plane strain is a special case, characterised by the lowest angle between the faults and the principal extension direction for any combination of rheology and flow type during progressive pure shear.

A model is proposed wherein the role of the anisotropy appears to be two-fold. First, it determines that shear bands operate internally by a mechanism involving rotating slip surfaces during fault nucleation. The initial orientation of the faults is determined by the optimisation of the driving processes in the propagating shear bands as a partial function of the angle they make with the external anisotropy. Second, it induces directionally dependent variation in the resistance to flow, which manifests itself differently according to the symmetry of the strain ellipsoid in three dimensions ($X \geq Y \neq 1 \geq Z$). In flattening flow, it is proposed that anisotropy-induced geometrical hardening leads to an increase in the angles made by the shear bands with the principal extension directions of the deformation. In constriction, the same effect is seen in *XZ* sections, but in *YZ* sections it is suggested that the wide range of fault orientations observed is due to anisotropy-induced geometrical softening.

It is possible that the low angle of dip of crustal-scale extensional detachment faults may reflect anisotropic behaviour of the lower continental crust.

Keywords: nucleating faults; three-dimensional deformation; rheology; anisotropy

1. Introduction

The nature and geometrical development of natural and experimental arrays of discrete faults has been examined by many workers in brittle (e.g., Aydin and Reches, 1982; Aydin and Johnson, 1983; Reches and Dieterich, 1983; Antonellini et al., 1994), ductile (e.g., Morgenstern and Tchalenko, 1967; Emmons, 1969; Logan et al., 1979, 1992), and plastic materials (e.g., Cloos, 1955; Oertel, 1965; Reches, 1988), who applied their analyses at all scales from intracrystalline dislocations (e.g., Lister and Williams, 1979; Law, 1990) to continental fault patterns (e.g., Nur et al., 1989; Garfunkel, 1989). Some workers have sought to determine the orientations of the principal strain rate axes of natural flow (e.g.,

* Corresponding author.

PII S0040-1951(96)00103-5

Arthaud, 1969; Angelier, 1979; Krantz, 1988, 1989; Twiss et al., 1991). Others have focused primarily on the relationship between the nature of the fault arrays and the symmetry of the bulk flow (e.g., Reches, 1978, 1983).

Most of the above cited studies address instantaneous flow, or an approximation to it (i.e. small magnitude finite strains), in homogeneous, isotropic media. Many, though not all, are limited to two dimensional plane strain. However, it is geologically axiomatic that many natural rocks are anisotropic, i.e. they are layered or contain a planar shape fabric. Indeed, one of the effects of progressive deformation is to impart an anisotropy, either in the form of a foliation, or a tectonic layering, to initially isotropic materials. Furthermore, it is also well established that flow can be three-dimensional (e.g., Ramsay, 1967, pp. 121–177; Ramberg, 1975), and that the shape of the strain ellipsoid can be described in terms of its symmetry, or shape (k value of Flinn, 1962). However, few studies of natural examples have specifically examined progressive three-dimensional deformation of anisotropic rocks, accommodated by slip on discrete shear planes (e.g., Mitra, 1979; Hanmer, 1979).

Since the initial work of Biot (e.g., Biot, 1965; see also Price and Cosgrove, 1990 and references therein), the influence of rheological anisotropy in deforming media has been theoretically and experimentally investigated (e.g., Paterson and Weiss, 1966; Donath, 1968; Cobbold et al., 1971; Williams and Means, 1971; Means and Williams, 1972; Cobbold, 1976; Cobbold and Watkinson, 1981; Latham, 1985a,b; Cobbold and Gapais, 1986; see also Williams and Price, 1990; Weijermars, 1992; Yin and Ranalli, 1992). However, many of these studies are concerned with two-dimensional plane strain, and most place their emphasis on layer-parallel shortening and the growth of folds. Two experimental studies which examine the case of layer-parallel extension in anisotropic media (Cobbold et al., 1971; Harris and Cobbold, 1985; see also Means and Williams, 1972) highlight a well known problem in fault mechanics. Theoretically, nascent conjugate faults in homogeneous, isotropic media are oriented with Z, the principal direction of shortening ($X \geq Y \geq Z$), parallel to the bisector of the acute angle between them. However, it is a common observation in anisotropic materials that the principal direction of shortening bisects the obtuse angle between the faults (e.g., Cobbold et al., 1971; Platt and Vissers, 1980; White et al., 1980; Behrmann, 1987; however, see Means and Williams, 1972). A comprehensive explanation of the potential role of the rheological anisotropy in influencing fault orientations has yet to be presented.

We have undertaken a set of simple physical experiments specifically designed to investigate the influence of planar rheological anisotropy on the orientation of fault structures in three-dimensional flow associated with layer-normal shortening. This contribution presents the results of bulk axially symmetrical flattening (layer-normal shortening; $X = Y > Z$), herein referred to simply as flattening, and bulk constriction ($X > Y = Z$) of finely layered plasticine–vaseline models. In what follows, we shall compare and contrast the behaviour of theoretical cohesive (e.g., Reches, 1978) and cohesive-frictional (Coulomb; e.g., Reches, 1983) model materials with that of experimental anisotropic plasticine–vaseline models, and draw upon them for an analogue to explain the behaviour of the anisotropic material.

We are well aware that isotropic Coulomb behaviour describes materials such as sand (e.g., Malavieille, 1984), and that pure cohesive behaviour describes essentially plastic materials (e.g., Ranalli, 1987). Neither is applicable to a work hardening, non-Newtonian material such as plasticine (McClay, 1976). Attempts to deform isotropic plasticine in a press such as ours are thwarted by the rapid rate of work hardening of the deforming material at relatively low finite strains, and sand is not the material of choice for constructing anisotropic models. Therefore, for all practical purposes, we are constrained to compare theoretical models for isotropic behaviour with experimental anisotropic models made of materials such as plasticine and vaseline. Accordingly, our results are only directly pertinent to our model materials. It is our hope that our results will catalyse further work more directly applicable to the three-dimensional deformation of natural anisotropic rocks.

It will be our hypothesis that the principal variable determining the differences in behaviour between isotropic and anisotropic materials is the rheologically active anisotropy, predicated on a shear band model of rotating anisotropy segments within the faults during their nucleation. Our experiments highlight the special character of initial fault orientations developed in anisotropic media subjected to plane strain, which we shall suggest may be explained in terms of a balance between those processes driving and those resisting the propagation of the fault tips. From comparison of our experiments with theoretical models for similar flows in both cohesive and Coulomb isotropic materials, we shall suggest that the orientation of the faults is also strongly influenced by an anisotropy-induced geometrical hardening (Poirier, 1980) with respect to layer-parallel extension in flattening, plus a geometrical softening with respect to layer-parallel shortening in constriction.

2. Experiments

2.1. Method

Model stacks, 15 by 15 by 30 cm, were constructed of hand-rolled layers of Harbutt's plasticine, approximately 1.5 mm thick, separated from each other by a thin film of petroleum jelly (Fig. 1A). Two colours of plasticine were used, yellow and plum, in order to create markers. Initial tests indicated no obvious viscosity difference between the two colours at room temperature. Accordingly, the models correspond to bilaminate plasticine–vaseline multilayers (Harris and Cobbold, 1985) whose anisotropic properties have been established by previous workers (e.g., Cobbold et al., 1971; Price and Cosgrove, 1990, chapter 13). It is also possible that rolling-induced alignment of plate-like grains of mineral filler within the plasticine (McClay, 1976) may impart a degree of anisotropy to the individual plasticine layers themselves (Peltzer, 1983).

The models were deformed in a simple steel press (Fig. 1B). The press contains four pistons made of 1 mm thick steel slats, resembling open venetian blinds. The pistons are arranged in two mutually perpendicular sets, with the slats of each piston alternating with those of its neighbours. Driven by hand-operated cranks, one set of pistons can move along the Y coordinate direction (X, Y and Z correspond to the principal strain axes $X \geq Y \geq Z$ in progressive pure shear), whereas the other set can move along Z. Accordingly, the pistons of each set can move along the direction normal to the piston face and pass through the pistons of the other set. The models are placed in the press with their rheological anisotropy oriented normal to Z. Inward displacement of all four pistons results in a constrictional flow ($k > 1$), with extrusion of material along X. Inward displacement of one set of pistons along Z and outward movement of the other set along Y results in flattening flows ($0 < k < 1$), where the extrusion along X only partially accommodates the shortening along Z. Penetration of the model material into the pistons is successfully avoided by wrapping the model in household wax paper. For constrictional experiments, a simple two-ply wax paper sleeve is applied over the XY and XZ faces of the model. The paper accommodates the change in surface area of these faces by very fine scale microcrenulations which do not propagate into the model itself. For flattening experiments, a similar sleeve is employed with the addition of a high-amplitude fold in the paper on the XY faces. As the surface area of these faces increases, the paper folds unravel and prevent tearing of the sleeve during deformation.

This experimental configuration suffers from several unavoidable drawbacks. First, we know of no practical way to construct a third set of flat-faced pistons which are rigid, capable of displacement along X, and able to accommodate surface area changes of the piston face. Therefore, in order to promote homogeneous extrusion, rigid Perspex endwalls are bolted to the external frame of the press. Prior to each small deformation increment, a gap of several millimetres is allowed between the endwalls and the YZ faces at each end of the model. During the deformation increment, the model extrudes across the gaps until it is pressed up against the endwalls. The endwalls are then slowly unbolted and removed, and the protruding volume of model material is cut away with the aid of a wire. Although this experimental procedure is polyaxial and progressive, it results in a discontinuous experimental deformation and variable strain rate. It is best described as an episodic, three-dimensional extrusion. As demonstrated by Means and Williams (1972), it also results in a degree of strain heterogeneity which we cannot control experimentally. However, the general reproducibility of the results (cf. Ganas, 1990) justifies the significance we attribute to them.

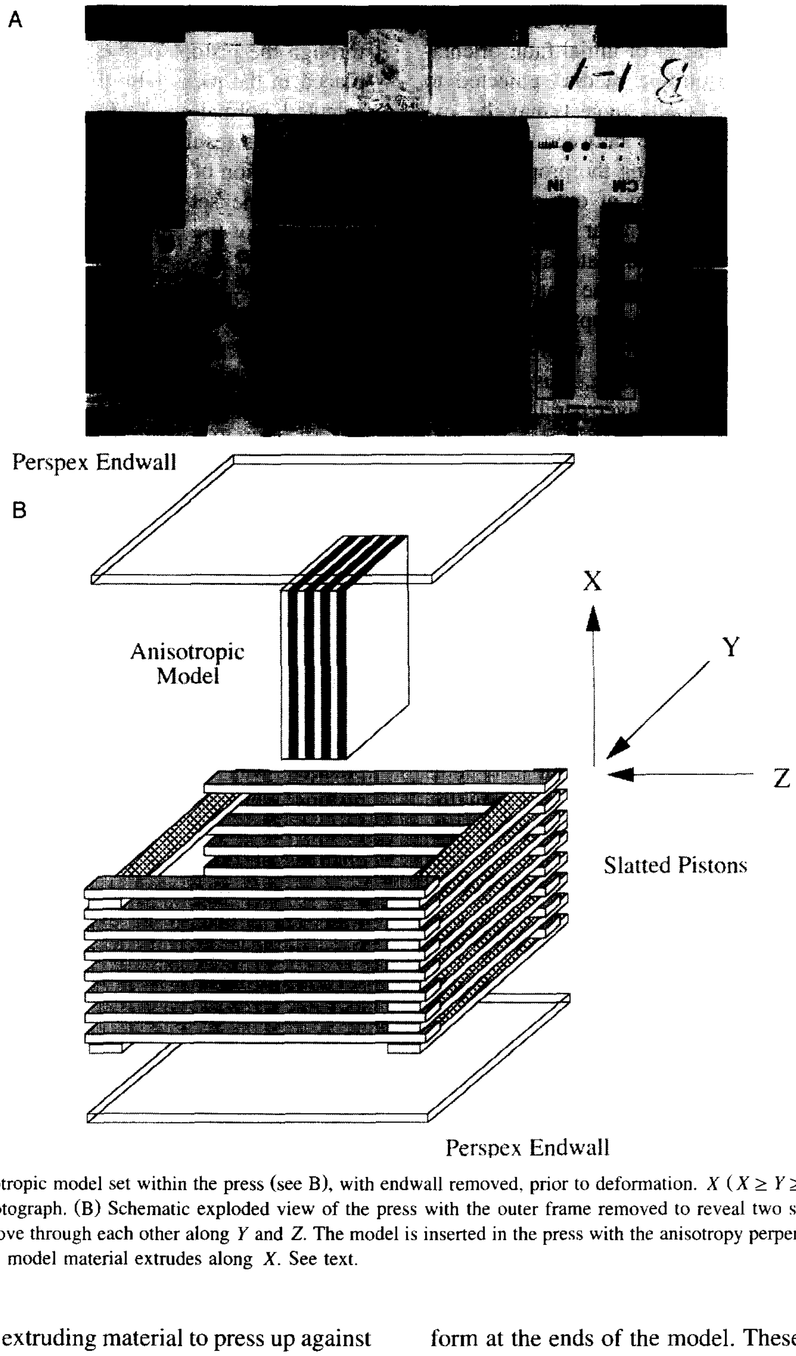

Fig. 1. (A) An anisotropic model set within the press (see B), with endwall removed, prior to deformation. X ($X \geq Y \geq Z$) perpendicular to the plane of the photograph. (B) Schematic exploded view of the press with the outer frame removed to reveal two sets of slatted pistons which are able to move through each other along Y and Z. The model is inserted in the press with the anisotropy perpendicular to Z. During the deformation, the model material extrudes along X. See text.

Allowing the extruding material to press up against the endwalls results in an end-effect which we have been unable to circumvent (see also Means and Williams, 1972). In XZ sections, "dead zones" form at the ends of the model. These are bounded by geometrically and kinematically complex zones which appear to have either initiated at, or propagated towards, the upper and lower faces of the models close to the endwalls, despite liberal lubrication with talc. This effect can be reduced by lowering the ambient temperature of the experiment, thereby increasing the overall strength of the model material. However, the viscosities of the two colours of plasticine do not show identical temperature sensitivities and the yellow layers are prone to boudinage when cooled. Therefore, we were unable to track the true evolution of the experimentally induced structures. Nevertheless, our measurements, taken from the interior of each model after post-experimental sectioning, can be compared qualitatively with observations made at the model ends during the experiments.

Plasticine has been used in many deformation experiments, including many of the studies cited in the Introduction. We chose to use it because it can be easily rolled and handled, and it is strong enough that the models do not flow when unsupported. Its rheological properties and composition are well enough known for our purpose (McClay, 1976; Dixon and Summers, 1985), i.e. it strain hardens sufficiently to enhance the development of discrete oblique slip planes, or shear bands (e.g., White et al., 1980). We have not sought to scale the models or the experimental conditions (e.g., Dixon and Summers, 1985; Treagus and Sokoutis, 1992).

Two sets of experiments were undertaken under constant flow regime. The first set corresponds to a flattening flow where up to 30% layer-normal shortening along the Z direction was accommodated by equal extensions along X and Y. The second set corresponds to a constrictional flow where up to 60% layer-parallel extension along the X direction resulted from equal shortening along Y and Z. Recognizing the heterogeneities in the deformation patterns adjacent to the piston faces, measurements were only taken from the central part of any given section.

3. Results

The observed angles made by the faults, measured in the principal sections of our flattening (Fig. 2 and Fig. 3) and constrictional experiments (Fig. 4 and Fig. 5) are presented in Fig. 6. Individual fault traces are straight, and few show detectable curvature at their terminations. From visual comparison of the deformed models with their initial states, we were unable to measure thinning of the individual plasticine layers. Although there is some rotation of some fault-bound blocks (Fig. 2B), it is localised and relatively minor, reflecting the alternation of oppositely dipping principal faults, as opposed to a domainal distribution of "bookshelf" fault arrays (e.g., Mandl, 1987), each with a single dip direction. Except for minor deflections near the piston surfaces, layer-parallel shortening in constrictional flow does not result in the initiation and amplification of buckle folds (Fig. 4A). We observed that most of the deformation was accommodated by slip along the experimentally-induced faults, with only a minor contribution from slip along the anisotropy in small localised volumes, fault rotation and thinning of layers. Moreover, taking the anisotropy as a marker, the similar

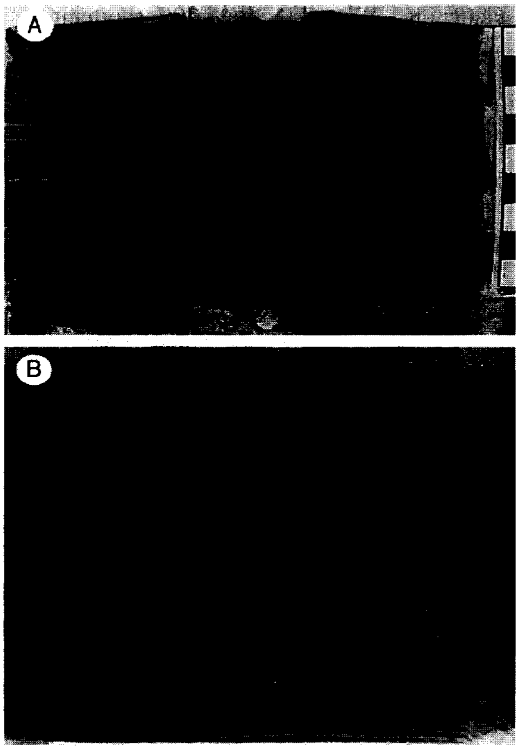

Fig. 2. YZ sections of model US3 subjected to flattening (30% layer-normal shortening along Z). (A) end section of model still set in press. (B) mid-section of model, note that external XZ slices have been removed. Scale in cm divisions. Refer to Fig. 3.

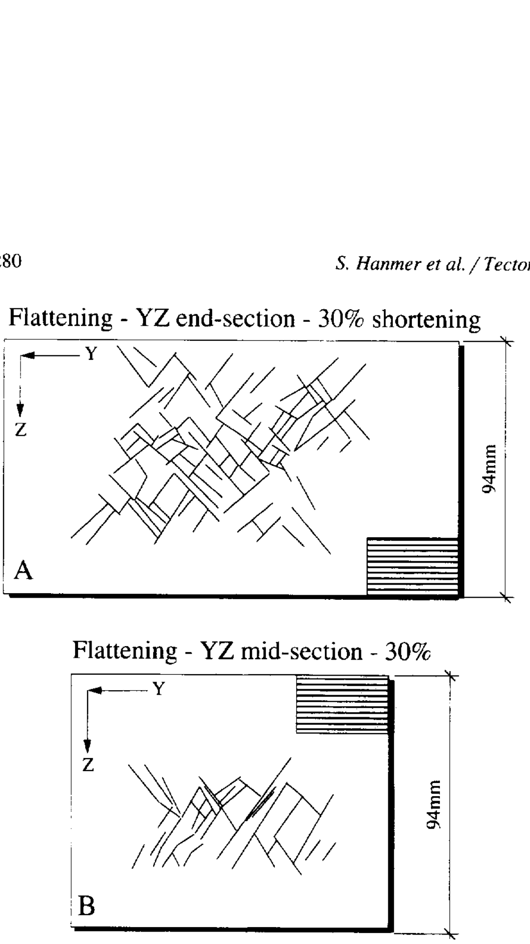

Fig. 3. Line segments traced from Fig. 2A (A) and B (B) of *YZ* sections of flattening experiment US3. Principal strain axes and the orientation of the anisotropy are indicated.

orientations of adjacent faults with widely different separations (apparent displacements), indicates that our data reflect the pattern of fault orientations at initiation (Figs. 2 and 4; see also Means and Williams, 1972).

The mean experimental fault orientations are presented as three-dimensional block diagrams (G and I in Fig. 7), along with the dihedral angle measured in the *XZ* plane for plane strain of anisotropic materials (H in Fig. 7; Cobbold et al., 1971). We also present the equivalent angles of fault initiation calculated from the theoretical isotropic models for cohesive materials (A–C in Fig. 7; Reches, 1978) and cohesive-frictional, i.e. Coulomb, materials (D–F in Fig. 7; Reches, 1983). There are clear differences in the patterns of initial fault orientation between the isotropic and anisotropic cases (compare A with G, and F with I, in Fig. 7). Referring to Figs. 6 and 7, we note the following salient points:

(1) In the *XZ* plane, the pattern of faults in the anisotropic material in flattening (G in Fig. 7) is very similar to that in constriction (I in Fig. 7), with a mean angle (α) of 49° with respect to the *X* direction.

(2) The *mean* fault orientations (β) in the anisotropic material are similar in the flattening and constrictional experiments; 49° and 47° with the *Y* direction, respectively (G and I in Fig. 7). However, whereas the clustering of fault orientations about the mean is pronounced in flattening, it is barely perceptible in constriction (Fig. 6).

(3) Combining our results with the data of Cobbold et al. (1971) for the case of plane strain, the simple variation in fault orientation from flattening to constrictional flows in isotropic materials, expressed as an increase in the angle (α) made with *X* in the *XZ* section, is not observed in the anisotropic material (Fig. 7). In the anisotropic case, the mean angle (α) is a minimum for plane strain ($k = 1$), and

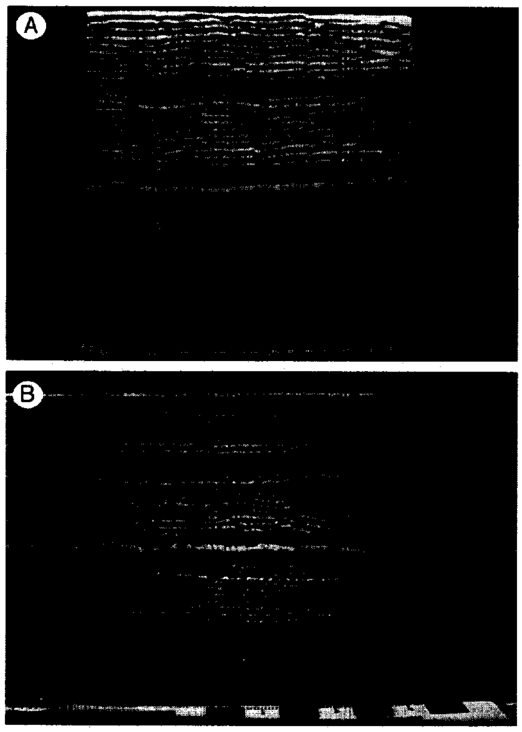

Fig. 4. *YZ* (A; *Y* is layer-parallel) and *XZ* (B; *X* is layer-parallel) sections cut through model ME1 subjected to constriction (60% layer-parallel extension along *X*). Scale in mm divisions in A, and cm divisions in B. Two vertical traces in A are cutting marks, not shears. Refer to Fig. 5.

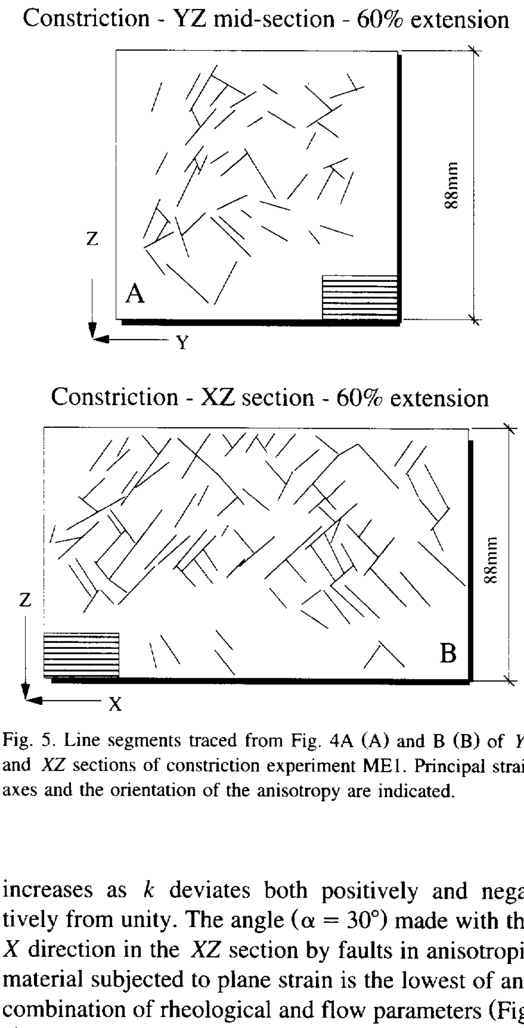

Fig. 5. Line segments traced from Fig. 4A (A) and B (B) of *YZ* and *XZ* sections of constriction experiment ME1. Principal strain axes and the orientation of the anisotropy are indicated.

increases as k deviates both positively and negatively from unity. The angle ($\alpha = 30°$) made with the X direction in the XZ section by faults in anisotropic material subjected to plane strain is the lowest of any combination of rheological and flow parameters (Fig. 7), indicating that plane strain in anisotropic materials is a special case.

Accordingly, while the relationship between fault orientation and pure shear flow type (k) in anisotropic materials differs from that in isotropic media, the influence of the anisotropy on the fault pattern is itself sensitive to k (Fig. 7). In flattening, the difference in fault orientation pattern is greatest between that in the anisotropic material and the theoretical cohesive model (compare G and A in Fig. 7). On the other hand the fault patterns in the anisotropic material and the theoretical Coulomb model are quite similar (compare G and D in Fig. 7). By contrast, in constrictional flow, the pattern of mean fault orientations in the anisotropic material is similar to the pattern predicted by the cohesive model (compare I and C in Fig. 7), but quite distinct from that of the Coulomb model (compare I and F in Fig. 7). In order to analyse these relationships, we first examine the variation in fault orientation patterns between the two sets of theoretical predictions for isotropic materials.

3.1. Frictional resistance to flow

Reches (1978, 1983) presented two variations of a theoretical model for the accommodation of homoge-

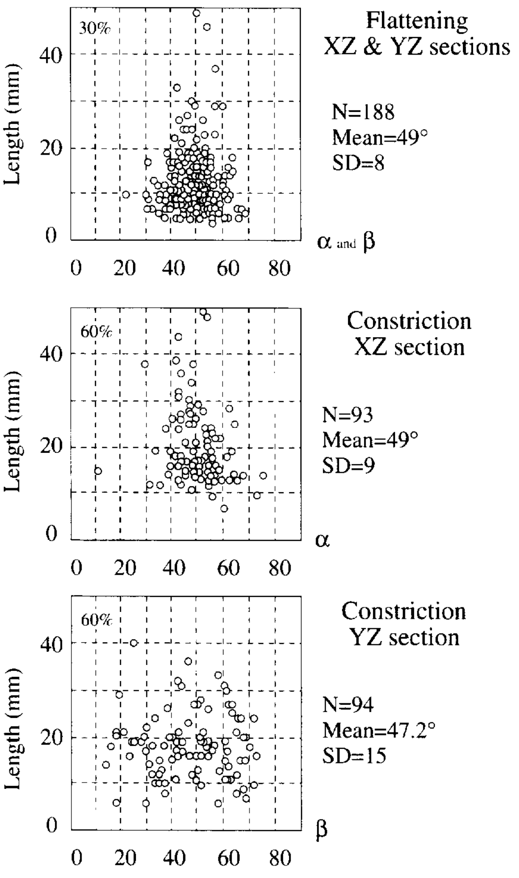

Fig. 6. Measured apparent angles (α or β) made by faults with the X (or Y) direction (see Fig. 7) in deformation experiments US3 and ME1, plotted against fault trace length. SD is standard deviation. The value of layer-normal shortening in flattening, or layer-parallel extension in constriction, is marked in the upper-left corner.

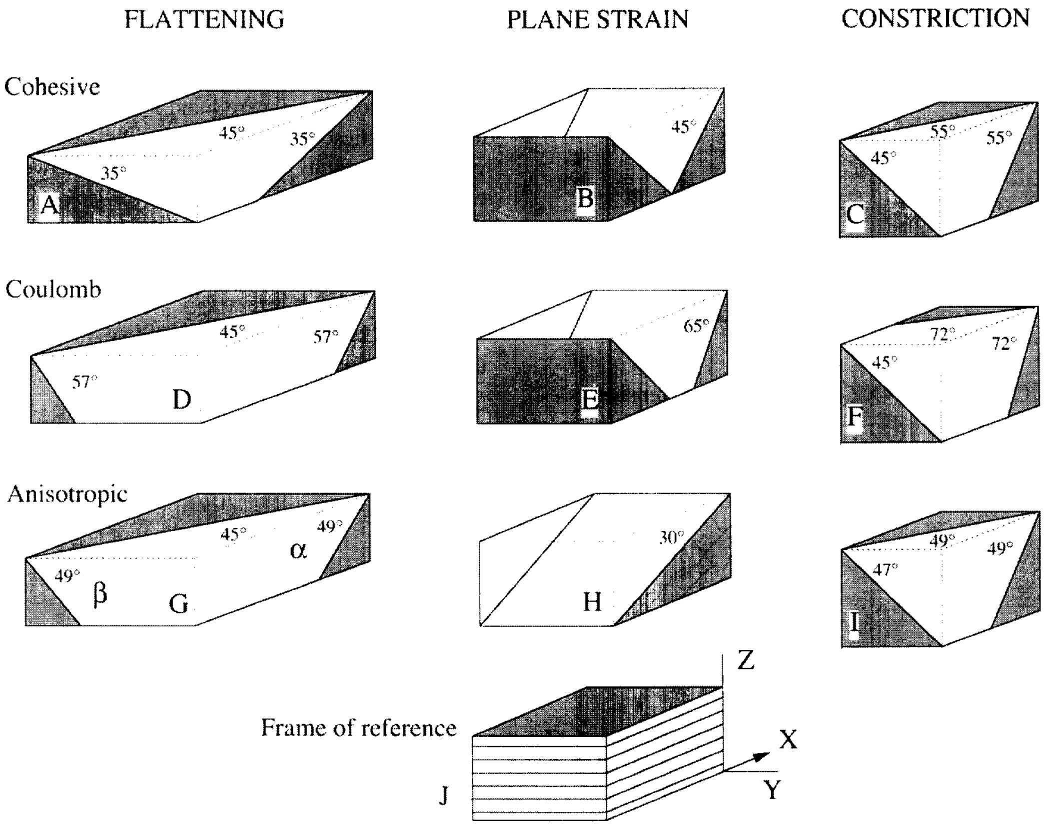

Fig. 7. Representation in 3D of apparent angles made by faults in theoretical isotropic models of cohesive (A–C) and Coulomb materials (D–F) in flattening, plane strain and constrictional flows, compared with their equivalents in experimental deformation of anisotropic models (G–I). The angle α and β, and the axes X, Y and Z are indicated, as is the orientation of the anisotropy in the models (J). Values on the top surfaces of each block refer to the angle to the right of the number. Note that the value of β in I is deceptive because it represents a very weak central tendency (see Fig. 6). Discussed in text.

neous three-dimensional bulk coaxial flow by arrays of discrete slip surfaces in isotropic materials, predicated on the following assumptions or constraints.

(1) Strain is accommodated by slip along faults.

(2) Fault slip is the sole deformation process.

(3) Resistance to slip along the faults is cohesive, or cohesive and frictional

(4) Faults which lead to minimum dissipation of mechanical energy are favoured.This last assumption is equivalent to applying the principle of minimum work done by external forces (Reches, 1978; see also Ramsay, 1967, pp. 436–456; Weiss, 1980). Note that the models are instantaneous, and only directly applicable to the initiation of slipping faults. This restriction does not detract from the utility of the models because post-initiation flow will be controlled by the presence of successfully nucleated faults attached to material points (e.g., Johnson, 1995). The nature of the resistance to fault slip depends upon the rheology of the material under consideration. Reches (1978) presented an initial model based upon cohesive resistance, subsequently refined with the addition of a frictional resistance (Reches, 1983). The first case is independent of the normal stress across the faults, in contrast to the second case which corresponds to classical Coulomb behaviour.

Two trends are immediately apparent in the fault patterns predicted by these models, and their variation with the shape of the strain ellipsoid (k; Fig. 7). The first, already noted above, is most simply expressed as an increase in the angle (α) made with X in the XZ section from flattening to constrictional flow (A → B → C and D → E → F in Fig. 7). The second is an increase in α for a given value of k when a linear component of frictional resistance is added to the cohesive strength of the material (compare A with D, B with E and C with F in Fig. 7). This relationship between fault orientation and frictional resistance to flow inspired us to examine rheologically anisotropic, non-frictional materials for *analogous* effects.

3.2. Anisotropy, hardening and softening

Rheological anisotropy can also influence the resistance of a material to flow. However, in contrast

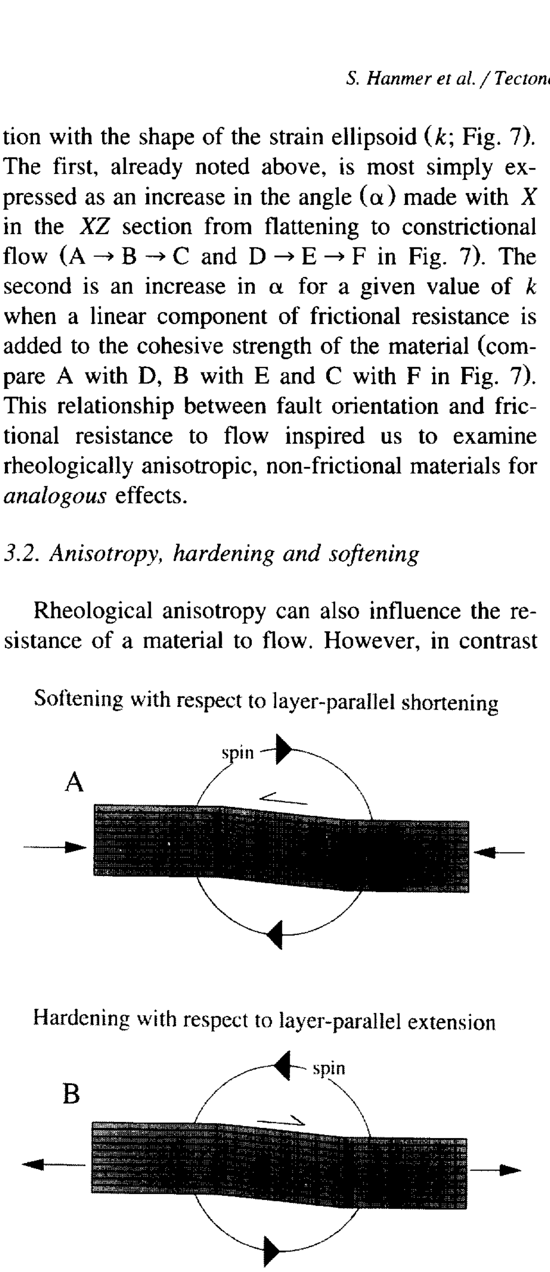

Fig. 8. Models of the manner in which rheological anisotropy can induce a geometrical softening or a geometrical hardening, depending upon the orientation of the anisotropy with respect to the principal stretching directions of the bulk flow. With respect to layer-parallel shortening (A), a local sinistral rotational flow resolved at the site of a pre-existing slipping anisotropy segment partitions to preferentially create spin (arrowed circle; Lister and Williams, 1983), enhancing the growth rate of the perturbation. With respect to layer-parallel extension (B), the locally created spin induces an anticlockwise rotation of the slipping anisotropy segment, thereby dampening the growth rate.

to friction, as well as all other potential sources of hardening and softening (e.g., Poirier, 1980), its effect is directionally dependent and may either weaken or strengthen the material. Treatments by Cobbold (Cobbold et al., 1971; Cobbold, 1976) and Poirier (1980) have established that rheological anisotropy can induce a geometrical softening, or a geometrical hardening, depending upon the orientation of the anisotropy with respect to the principal stretching directions of the bulk flow, tending to either enhance or suppress the amplification of perturbations. Simple models interpreting the role of the anisotropy are presented in Fig. 8. A local rotational flow induced at the site of a pre-existing low-amplitude perturbation in a planar anisotropy subjected to layer-parallel shortening can partition to preferentially create spin (Lister and Williams, 1983), at least initially. In the example shown (Fig. 8A), the spin enhances the passive component of amplification of the perturbation (Turner and Weiss, 1963, pp. 383, 384), thereby accelerating the growth rate of the developing structure. By similar reasoning, spin induced at a pre-existing perturbation in an anisotropic material subjected to layer-parallel extension can hasten the decrease in amplitude of the perturbation (Fig. 8B), thereby increasing the resistance to flow (e.g., Biot, 1965).

4. Discussion

When the fault orientation patterns produced by the experimental deformation of a rheologically anisotropic material are compared with those predicted for isotropic materials, we observe a rather complex set of differences which vary with the flow type (k; Fig. 7). The influence of a rheological anisotropy on the fault patterns is not the same in the three flow types examined here. Indeed, when superficially compared with the rather simple effect of introducing a component of frictional resistance into cohesive isotropic materials, the influence of a rheological anisotropy appears contradictory from one flow type to another. However, as already noted, the hardening or softening effect of a rheological anisotropy is directionally dependent. Therefore, we now consider the role of the anisotropy with respect to flow along the principal stretching axes in the XY plane in flattening, constriction and plane strain.

The principal effects of a rheological anisotropy are the canalisation of slip, and the variable partitioning of the flow in multilayers (Lister and Williams, 1983), sometimes referred to as strain refraction (e.g., Treagus, 1988). Deformation of a material with a strong planar anisotropy tends to be accommodated by the formation of band-like structures with short limbs composed of rotating segments of slipping anisotropy (e.g., Cobbold et al., 1971; Means and Williams, 1972). The influence of anisotropy on fault patterns suggests relationships between fault orientation, rate of fault propagation, and efficient operation of the dominant deformation mechanism within the fault, which influence successful nucleation and growth. Accordingly, this discussion will focus on the role of the anisotropy in the nucleation of the faults, predicated on a physical model of an incipient fault with a finite thickness and an internally anisotropic structure, i.e. a shear band (Fig. 9; White et al., 1980). Because a successfully nucleated fault is attached to material points, it is the initiation stage which controls the orientation of the maturing structure, independent of probable post-initiation changes in deformation mechanism (see also Means and Williams, 1972). We have already noted that the fault pattern associated with anisotropic materials subjected to plane strain appears to be a special case. We therefore begin this discussion by considering the possible role of rheological anisotropy in determining the initial fault orientation pattern in plane strain. We shall then propose a hypothesis whereby the directionally dependent hardening/softening effect of the anisotropy further influences the fault orientation pattern in three-dimensional flow relative to the two-dimensional plane strain ground state.

4.1. Plane strain

From kinematic analysis of layer-parallel shortening in anisotropic materials subjected to plane strain, Ramsay (1967, pp. 436–456) showed that the geometries of chevron folds and compressional kink

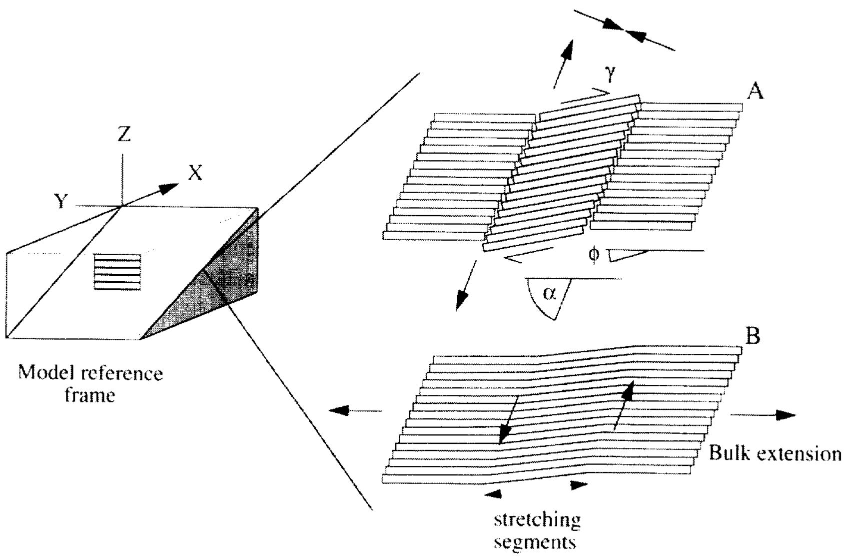

Fig. 9. Models of a discrete shear band of rotating, actively slipping layer segments and their setting with respect to a fault in the experimental model reference frame. (A) If the length of the rotating anisotropy segments within the shear band is invariant, the width of the band decreases (convergent arrows) as the segments rotate, and the band boundary increases in length (unmarked divergent arrows). (B) A stretching bookshelf shear zone set in the same frame of reference as A. The internal rotating segments extend to maintain constant width of the shear zone and ensure a simple shear regime parallel to the zone margin. γ is shear strain on the slipping rotating segments, ϕ is the rotation of the segments and α is the angle between the shear band boundary and the bulk extension direction (X) in the XZ plane of the reference frame. Note that, for drafting purposes and clarity, the angle α has been greatly exaggerated.

bands tend toward those predicted from consideration of the variation of shear strain increments ($d\gamma/de$) with variation in total layer-parallel shortening of the deforming system. In brief, the classical "ideal" kink and chevron geometries (Paterson and Weiss, 1966) are those for which the shear strain (γ) increments on the slipping and rotating anisotropy, within the kink, are minimal for a given increment of bulk layer-parallel shortening (e). This is equivalent to the application by Reches (1978, 1983) of the principle of minimum dissipation of mechanical energy.

Dewey (1965) applied similar kinematic analysis to extensional shear band-like structures in anisotropic materials based on a model of discrete planar shear zones composed of rotating, antithetically slipping layer segments (Fig. 9A). A subsequent comprehensive analysis of the behaviour of arrays of rotating parallel faults in progressive plane strain (e.g., Freund, 1974; Garfunkel and Ron, 1985; Garfunkel, 1989; Nur et al., 1989) is analogous to that of Dewey (1965). These models allow quantitative derivation of a number of potentially useful relationships as a function of the angle made by the internal anisotropy segments with the shear band boundaries: (1) propagation of the shear band by stretching of the shear band boundary with rotation of the internal anisotropy; and (2) incremental shear strain on the rotating anisotropy with progressive bulk deformation. However, because the models treat the length of the rotating anisotropy segments within the shear band as invariant (Fig. 9A), the width of the band must decrease as the segments rotate. Unless the rotating segments increase in length with progressive deformation (e.g., Lister and Williams, 1983), such a model cannot lead to bulk extension in the directions observed in our experiments (see also Cobbold et al., 1971). However, in contrast to experimental observation (Fig. 7H), this stretching bookshelf mechanism would favour shear bands making high angles (α) with the external anisotropy in order to minimise the extension of the rotating segments required to maintain shear band width (Fig. 9B; Mandl, 1987).

Alternatively, slip on the internal anisotropy may be synthetic with respect to displacement across the shear band. Like all active shear zones, shear bands propagate at their tips in order to accommodate the displacement across their central sections (e.g., Ramsay, 1980; Simpson, 1983; Ingles, 1986). Because synthetic slip is more readily activated on planes which make a low angle with respect to the bulk flow plane (e.g., Berthé et al., 1979; Williams and Price, 1990; Hanmer and Passchier, 1991, fig. 36), the rate of slip on the internal anisotropy segments, and therefore the rate of shear band propagation, will be greater than in high-angle shear bands. Successful propagation of a shear band requires that work be done to overcome the initial resistance of the anisotropy to slip at the shear band tips. However, the rate of rotation of the anisotropy within a shear band is also a partial function of the orientation of the shear band boundary with respect to the external anisotropy (α; Fig. 9); faster for high angles and slower for low angles (Garfunkel and Ron, 1985). Together, these relationships suggest that (1) rotation of anisotropy segments might not be effective in accommodating the propagation rates of low-angle shear bands and (2) that the propagation rates of high angle shear bands may be too slow to accommodate the imposed bulk strain rate. If this interpretation is valid, it further suggests that the disposition of shear bands observed in plane strain ($\alpha = 30°$) is an intermediate orientation representing a balance between processes driving and processes resisting shear band growth, specific to that flow type.

4.2. Flattening and constriction

The angles α and β in the fault orientation pattern produced in our experimental flattening deformation of anisotropic material (G in Fig. 7) are greater than those predicted for the same flow symmetry in cohesive isotropic materials (A in Fig. 7). By analogy with the effect produced by the addition of a linear frictional resistance in isotropic materials (compare A and D in Fig. 7), we suggest that the presence of an anisotropy confers an additional resistance, i.e. a geometrical hardening with respect to layer-parallel extension (Fig. 8). Because the shortening along Z in axially symmetrical flattening is accommodated by equal extensions along the X and Y directions, the angles made by the faults with X (α in XZ section) and Y (β in YZ section) are identical (Fig. 7). Hence, according to our interpretation, the geometrical hardening due to the presence of an anisotropy is manifested by equal increases in both α and β. However, useful as it is, this analogy is not without its limitations. First, when compared with isotropic materials, the introduction of a rheological anisotropy does not result in an increase in a in the case of plane strain (Fig. 7; see above). Second, the increase in α and β in anisotropic materials with change in flow type (compare G and H in Fig. 7), suggests that the hardening effect is variable within materials of similar degree of anisotropy. However, before pursuing these observations, we must first examine the case of constrictional flow. Because layer-parallel extension is accompanied by layer-parallel shortening, the situation is more complex in constriction than for either flattening or plane strain flow. There are two important observational points to be made.

First, there is a potential geometrical softening effect with respect to layer-parallel shortening along the Y direction in the anisotropic material (compare I in Fig. 7 with Fig. 8). The mean fault orientation (β = ca. 47°) in the YZ section, essentially indistinguishable from that for either of the isotropic cases (45°), is simply a reflection of the axial symmetry of the extension. However, the poor clustering of the fault orientations (Fig. 6) is significant. The broadening of the spread of fault orientations compared with the isotropic models could be considered as a relaxation of Reches' fourth assumption or constraint, i.e. that faults which lead to minimum dissipation of mechanical energy are favoured (see above). Following this line of reasoning, we suggest that geometrical softening with respect to layer-parallel shortening along Y (Fig. 8) might enhance the ability of a range of otherwise less than ideally oriented, internally anisotropic shear bands to nucleate, thereby widening the range of energetically efficient fault orientations.

Second, there is a potential geometrical hardening effect with respect to layer-parallel extension along the X direction (compare I in Fig. 7 with Fig. 8). However, comparison of the fault patterns in the XZ section between the anisotropic and the cohesive isotropic cases shows little difference, and therefore no apparent evidence for such hardening (compare C and I in Fig. 7). In our experiments the fault pattern in the XZ section in constriction is identical to that in the XZ and YZ sections in flattening (see Figs. 6 and 7), and α is always smaller than that predicted for Coulomb isotropic materials (compare G with D and I with F in Fig. 7). We speculate that the maximum angle (α = ca. 50°) observed in all of our experiments represents the limit at which the propagation rate of the shear bands is the minimum for successful nucleation in a rheologically anisotropic medium. If valid, this would explain why α is not a good marker of the anisotropy-induced geometrical hardening effect in constrictional flows when $k \gg 1$.

Compared with flattening and constrictional flow, α is much smaller in plane strain (H in Fig. 7). We cannot adequately explain this variation in fault orientation with flow type. Empirically, given the equivalence of layer-normal shortening and layer-parallel extension, it would appear that the geometrical hardening effect of the rheological anisotropy is enhanced by ratios of absolute values of finite strain parallel to X and Y which deviate either positively or negatively from unity.

In brief, we hypothesise that the role of a rheological anisotropy is two-fold. First, it determines that shear bands operate internally by a mechanism involving rotating slip surfaces during fault nucleation, thereby determining the initial orientation of faults in plane strain. Second, it induces directionally dependent variation in resistance to flow. In flattening flow, anisotropy-induced geometrical hardening (Fig. 8) leads to an increase in the angles made by shear bands with the X (α) and Y (β) directions (30° vs. ca. 50°; compare G and H in Fig. 7). The same effect with respect to α is apparent in the XZ section of constrictional flow (compare H and I in Fig. 7), but is not obvious from comparison with the isotropic materials in which α is greater than the maximum values possible for the shear band model (ca. 50°; compare C and F with I in Fig. 7). In the YZ section of constrictional flow, anisotropy-induced geometrical softening leads to a broadening of the range of energetically favourable fault orientations, compared with isotropic materials (Figs. 6 and 7C, F). In plane strain, the orientation of faults is a function of two competing influences: (1) optimisation of driving processes in growing shear bands; and (2) geometrical hardening due to layer-parallel extension. Comparison with the theoretical predictions of the isotropic models suggests that the former influence dominates in plane strain.

5. Comparison with natural structures

The results of our deformation experiments serve to illustrate the effects of geometrical hardening and softening due to the presence of a rheological anisotropy in three-dimensional flow. In our analysis, the role of the anisotropy is only strictly applicable to the nucleation of structures which accommodate the bulk shape change of the deforming material. Few published studies specifically address natural arrays of shear bands associated with three-dimensional strain (Hanmer, 1979; Mitra, 1979). However, a great deal of attention has been focused on the orientation of extensional detachment faults and their footwall mylonites, which characteristically dip at ca. 25–30° or less (e.g., Davis, 1988; Davis and Lister, 1988). The low angle made by the faults with the directions of bulk principal strain has generated much debate regarding the initiation of such structures. If detachment faults are *stress controlled*, they lie in a most unfavourable orientation for frictional slip (Sibson, 1985; Scott and Lister, 1992). Some have therefore suggested that they initiated as low-angle thrusts (e.g., Malavieille, 1987; see also discussion in Davis and Lister, 1988). Others have proposed various models to rotate the stress field with respect to the faults by mid-crustal magmatic inflation (Parsons and Thompson, 1993), a mid-crustal stress guide (Lister and Davis, 1989), or crustal and/or lithospheric flexure (Spencer and Chase, 1989; Forsyth, 1992; Buck, 1993).

We suggest that anisotropic behaviour of the continental crust may be an important factor, hitherto ignored in the debate over detachment fault initiation (cf. Lister and Davis, 1989). Detachment faults are, by definition, large-scale structures (Davis and Lister, 1988). Accordingly they may be considered at the crustal-scale (e.g., Carr et al., 1987; Cook et al., 1992). At middle to lower crustal levels, faults are manifested as plastic shear zones (e.g., Hanmer, 1988). It is therefore possible to treat the upper, frictional parts of faults as the *kinematically controlled* brittle expression of crustal displacements (cf. Lister and Davis, 1989). Furthermore, as geometrically simple, laterally extensive, narrow zones of dip-slip displacement separating relatively stiff wallrocks, they form under conditions of bulk plane strain, and resemble the faults experimentally obtained in anisotropic materials (H in Fig. 7). It is clear that large volumes of the crust are neither layered nor rheologically anisotropic (e.g., Pitcher, 1978; Atherton, 1990; Paterson and Fowler, 1993). However, there is abundant geophysical and geological evidence for the lithologically layered nature of large volumes of the continental crust (e.g., Hall, 1986; Blundell, 1990; Warner, 1990; Holbrook et al., 1991; Mooney and Meissner, 1992; Lucas and St-Onge, 1995). Accordingly, our analysis of deformation in anisotropic materials suggests that detachment faults *should* initiate at ca. 30°.

6. Conclusions

In anisotropic materials subjected to layer-normal shortening, plane strain appears to be a special case. We hypothesise that the role of the anisotropy is two-fold: (1) It determines that shear bands operate internally by a mechanism involving rotating slip surfaces during fault nucleation. The initial orientation of the faults is determined by the optimisation of the driving processes in the propagating shear bands as a partial function of the angle they make with the external anisotropy. (2) It induces directionally dependent variation in resistance to flow, which manifests itself differently according to the flow type. The low angle of dip of crustal-scale extensional detachment faults may reflect anisotropic behaviour of the lower continental crust.

Acknowledgements

This work, undertaken at Carleton University, was funded by a Natural Science and Engineering Research Council grant to SH. P. Cobbold was instrumental, in both deed and word, in kindling our initial interest in the deformation of anisotropic materials, many years ago when SH was a Post-Doctoral Fellow at Rennes, France. F. Schwerdtner kindly loaned us the press, built at University of Toronto by H. Hugon, based on the original model designed by P. Cobbold. We are indebted to S. Lucas, W. Means, G. Ranalli and M. Williams for carefully and critically reading an initial draft of the manuscript. We also wish to thank our formal reviewers, particularly P. Williams, for their insightful and helpful comments. This is Geological Survey of Canada contribution #24895.

References

Angelier, J., 1979. Determination of the mean principal directions of stresses for a given fault population. Tectonophysics, 56: T17–T26.

Antonellini, M.A., Aydin, A. and Pollard, D.D., 1994. Microstructure of deformation bands in porous sandstones at Arches National Park, Utah. J. Struct. Geol., 16: 941–959.

Arthaud, F., 1969. Méthode de détermination graphique des directions d'allongement, de raccourcissement et intermédiaire d'une population de failles. Bull. Soc. Géol. Fr., 11: 729–737.

Atherton, M.P., 1990. The Coastal Batholith of Peru: the product of rapid recycling of "new" crust formed within rifted continental margin. Geol. J., 25: 337–349.

Aydin, A. and Johnson, A.M., 1983. Analysis of faulting in porous sandstones. J. Struct. Geol., 5: 19–35.

Aydin, A. and Reches, Z., 1982. Number and orientation of fault sets in the field and in experiments. Geology, 10: 107–112.

Behrmann, J.H., 1987. A precautionary note on shear bands as kinematic indicators. J. Struct. Geol., 9: 659–666.

Berthé, D., Choukroune, P. and Jegouzo, P., 1979. Orthogneiss, mylonite and non-coaxial deformation of granites: the example of the South Armorican shear zone. J. Struct. Geol., 1: 31–42.

Biot, M.A., 1965. Mechanics of Incremental Deformations. Wiley, New York, 504 pp.

Blundell, D.J., 1990. Seismic images of continental lithosphere. J. Geol. Soc. London, 147: 895–913.

Buck, W.R., 1993. Effect of lithospheric thickness on the formation of high- and low-angle normal faults. Geology, 21: 933–936.

Carr, S.D., Parrish, R.R. and Brown, R.L., 1987. Eocene structural development of the Valhalla Complex, southeastern British Columbia. Tectonics, 6: 175–196.

Cloos, E., 1955. Experimental analysis of fracture patterns. Geol. Soc. Am. Bull., 66: 241–256.

Cobbold, P.R., 1976. Mechanical effects of anisotropy during large finite deformation. Bull. Soc. Géol. Fr., 17: 1497–1510.

Cobbold, P.R., Cosgrove, J.W. and Summers, J.M., 1971. Development of internal structures in deformed anisotropic rocks. Tectonophysics, 12: 23–53.

Cobbold, P.R. and Gapais, D., 1986. Slip-system domains: I: Plane-strain kinematics of arrays of coherent bands with twinned fibre orientations. Tectonophysics, 131: 113–132.

Cobbold, P.R. and Watkinson, A.J., 1981. Bending anisotropy: a mechanical constraint on the orientation of fold axes in an anisotropic medium. Tectonophysics, 72: T1–T10.

Cook, F.A., Varsek, J.L., Clowes, R.M., Kanasewich, E.R., Spencer, C.S., Parrish, R.R., Brown, R.L., Carr, S.D., Johnson, B.J. and Price, R.A., 1992. Lithoprobe crustal reflection cross section of the southern Canadian Cordillera, 1 Foreland thrust and fold belt to Fraser River Fault. Tectonics, 11: 12–35.

Davis, G.A., 1988. Rapid upward transport of mid-crustal mylonitic gneisses in the footwall of a Miocene detachment fault, Whipple Mountains, southeastern California. Geol. Rundsch., 77: 191–209.

Davis, G.A. and Lister, G.S., 1988. Detachment faulting in continental extension: Perspectives from the Southwestern U.S. Cordillera. Geol. Soc. Am. Spec. Pap., 218: 133–159.

Dewey, J.F., 1965. Nature and origin of kink bands. Tectonophysics, 1: 459–494.

Dixon, J.M. and Summers, J.M., 1985. Recent developments in centrifuge modelling of tectonic processes, equipment, model construction techniques and rheology of model material. J. Struct. Geol., 7: 83–102.

Donath, F.A., 1968. Experimental study of kink band development in Martinsburg Slate. In: A.J.B.D.K. Norris (Editor), Kink Bands and Brittle Deformation. Geol. Surv. Canada, Ottawa, pp. 255–287.

Emmons, R.C., 1969. Strike-slip rupture patterns in sand models. Tectonophysics, 7: 71–87.

Flinn, D., 1962. On folding during three-dimensional progressive deformation. Q. J. Geol. Soc. London, 118: 385–433.

Forsyth, D.W., 1992. Finite extension and low-angle normal faulting. Geology, 27–30.

Freund, R., 1974. Kinematics of transform and transcurrent faults. Tectonophysics, 21: 93–134.

Ganas, A., 1990. Three-dimensional Deformation of a Statistically Homogeneous Anisotropic Material at High Strains, by Formation of Extensional Ductile Shears. MSc Thesis, Carleton University (unpublished).

Garfunkel, Z., 1989. Regional deformation by block translation and rotation. In: C. Kissel and C. Laj (Editors), Paleomagnetic Rotations and Continental Deformation. Kluwer, Dordrecht, pp. 181–208.

Garfunkel, Z. and Ron, H., 1985. Block rotation and deformation by strike-slip faults. 2. The properties of a type of macrospcopic discontinuous deformation. J. Geophys. Res., 90: 8589–8602.

Hall, J., 1986. The physical properties of layered rocks in deep continental cust. In: J.B. Dawson, D.A. Carswell, J. Hall and K.H. Wedepohl (Editors), The Nature of the Lower Continental Crust. Geol. Soc., pp. 51–62.

Hanmer, S., 1979. The role of discrete heterogeneities and linear fabrics in the formation of crenulations. J. Struct. Geol., 1: 81–91.

Hanmer, S., 1988. Great Slave Lake Shear Zone, Canadian Shield: reconstructed vertical profile of a crustal-scale fault zone. Tectonophysics, 149: 245–264.

Hanmer, S. and Passchier, C.W., 1991. Shear-sense indicators: a review. Geol. Surv. Can. Pap., 90-17, 72 pp.

Harris, L.B. and Cobbold, P.R., 1985. Development of conjugate shear bands during bulk simple shearing. J. Struct. Geol., 7: 37–44.

Holbrook, W.S., Catchings, R.D. and Jarchow, C.M., 1991. Origin of deep crustal reflections: Implications of coincident seismic refraction and reflection data in Nevada. Geology, 19: 175–179.

Ingles, J., 1986. Terminations of ductile shear zones. Tectonophysics, 127: 87–95.

Johnson, A.M., 1995. Orientations of faults determined by premonitory shear zones. Tectonophysics, 246: 161–238.

Krantz, R.L., 1989. Orthorhombic fault patterns: the odd axis model and slip vector orientations. Tectonics, 8: 483–495.

Krantz, R.W., 1988. Multiple fault sets and three-dimensional strain: theory and application. J. Struct. Geol., 10: 225–237.

Latham, J.P., 1985. The influence of nonlinear material properties and resistance to bending on the development of internal structures. J. Struct. Geol., 7: 225–236.

Latham, J.P., 1985. A numerical investigation and geological discussion of the relationship between folding, kinking and faulting. J. Struct. Geol., 7: 237–249.

Law, R.D., 1990. Crystallographic fabrics: a selective review of their application to research in structural geology. In: R.J. Knipe and E.H. Rutter (Editors), Deformation Mechanisms, Rheology and Tectonics. Geol. Soc. London, pp. 335–352.

Lister, G.S. and Davis, G.A., 1989. The origin of metamorphic core complexes and detachment faults formed during Tertiary continental extension in the northern Colorado River region, U.S.A. J. Struct. Geol., 11: 65–94.

Lister, G.S. and Williams, P.F., 1979. Fabric development in shear zones: theoretical controls and observed phenomena. J. Struct. Geol., 1: 283–298.

Lister, G.S. and Williams, P.F., 1983. The partitioning of deformation in flowing rock masses. Tectonophysics, 92: 1–33.

Logan, J.M., Dengo, C.A., Higgs, N.G. and Wang, Z.Z., 1992. Fabrics of experimental fault zones: their development and relationship to mechanical behaviour. In: B. Evans and T.F. Wong (Editors), Fault Mechanics and Transport Properties of Rocks: A Festschrift in Honor of W.F. Brace. Academic Press, New York, pp. 33–67.

Logan, J.M., Friedman, M., Higgs, N.G., Dengo, C. and Shimamoto, T., 1979. Experimental studies of simulated gouge and their application to studies of natural fault zones. In: Proc. 8th Conf. Analysis of Actual Faults in Bedrock, pp. 305–343.

Lucas, S.B. and St-Onge, M.R., 1995. Syn-tectonic magmatism and the development of compositional layering, Ungava Orogen (northern Quebec, Canada). J. Struct. Geol., 17: 475–491.

Malavieille, J., 1984. Modélisation expérimentale des chevauchements imbriqués: application aux chaines de montagnes. Bull. Soc. Géol. Fr., 26: 129–138.

Malavieille, J., 1987. Kinematics of compressional and extensional ductile shearing deformation in a metamorphic core complex of the northeastern Basin and Range. J. Struct. Geol., 9: 541–554.

Mandl, G., 1987. Tectonic deformation by rotating parallel faults: the "bookshelf" mechanism. Tectonophysics, 141: 277–316.

McClay, K.R., 1976. The rheology of plasticine. Tectonophysics, 33: T7–T15.

Means, W.D. and Williams, P.F., 1972. Crenulation cleavage and faulting in an artificial salt–mica schist. J. Geol., 80: 569–591.

Mitra, G., 1979. Ductile deformation zones in the Blue Ridge basement rocks and estimation of finite strains. Geol. Soc. Am. Bull., 90: 935–951.

Mooney, W.D. and Meissner, R., 1992. Multi-genetic origin of crustal reflectivity: a review of seismic reflection profiling of the continental lower crust and Moho. In: D.M. Fountain, R.J. Arculus and R.W. Kay (Editors), Continental Lower Crust. Elsevier, Amsterdam, pp. 45–79.

Morgenstern, N.R. and Tchalenko, J.S., 1967. Microstructural observations on shear zones from slips in natural clays. In: Proc. Geotech. Conf., Oslo, 1967, 1: 147–152.

Nur, A., Ron, H. and Scotti, O., 1989. Mechanics of distributed fault and block rotation. In: C. Kissel and C. Laj (Editors), Paleomagnetic Rotations and Continental Deformation. Kluwer, Dordrecht, pp. 209–228.

Oertel, G., 1965. The mechanism of faulting in clay experiments. Tectonophysics, 2: 343–393.

Parsons, T. and Thompson, G.A., 1993. Does magmatism influence low-angle faulting? Geology, 21: 247–250.

Paterson, M.S. and Weiss, L.E., 1966. Experimental deformation and folding in phyllite. Geol. Soc. Am. Bull., 77: 343–374.

Paterson, S.R. and Fowler, T.K., 1993. Re-examining pluton emplacement processes. J. Struct. Geol., 15: 191–206.

Peltzer, G., 1983. Naissance et Évolution des Décrochements lors d'une Collision Continentale: Approche Expérimentale et Application à la Tectonique de l'Est de l'Asie. Thesis, Université de Paris VII (unpublished).

Pitcher, W.S., 1978. Anatomy of a batholith. J. Geol. Soc. London, 135: 157–182.

Platt, J.P. and Vissers, R.L.M., 1980. Extensional structures in anisotropic rocks. J. Struct. Geol., 2: 397–410.

Poirier, J.P., 1980. Shear localisation and shear instability in materials in the ductile field. J. Struct. Geol., 2: 135–142.

Price, N.J. and Cosgrove, J.W., 1990. Analysis of Geological Structures. Cambridge University Press, Cambridge, 502 pp.

Ramberg, H., 1975. Particle paths, displacement and progressive strain applicable to rocks. Tectonophysics, 28: 1–37.

Ramsay, J.G., 1967. Folding and Fracturing of Rocks. McGraw Hill, New York, pp. 568.

Ramsay, J.G., 1980. Shear zone geometry: a review. J. Struct. Geol., 2: 83–99.

Ranalli, G., 1987. Rheology of the Earth, deformation and flow processes in geophysics and geodynamics. Allen and Unwin, Boston, 366 pp.

Reches, Z., 1978. Analysis of faulting in a three dimensional strain field. Tectonophysics, 47: 109–129.

Reches, Z., 1983. Faulting of rocks in three-dimensional strain fields II. Theoretical analysis. Tectonophysics, 95: 133–156.

Reches, Z., 1988. Evolution of fault patterns in clay experiments. Tectonophysics, 145: 141–156.

Reches, Z. and Dieterich, J.H., 1983. Faulting of rocks in three-dimensional strain fields I. Failure of rocks in polyaxial, servo-control experiments. Tectonophysics, 95: 111–132.

Scott, R.J. and Lister, G.S., 1992. Detachment faults: Evidence for a low angle origin. Geology, 20: 833–836.

Sibson, R.H., 1985. A note on fault reactivation. J. Struct. Geol., 7: 751–754.

Simpson, C., 1983. Displacement and strain patterns from naturally occurring shear zone terminations. J. Struct. Geol., 5: 497–506.

Spencer, J.E. and Chase, C.G., 1989. Role of crustal flexure in initiation of low-angle normal faults and implications for structural evolution of the Basin and Range Province. J. Geophys. Res., 94: 1765–1775.

Treagus, S.H., 1988. Strain refraction in layered systems. J. Struct. Geol., 10: 517–527.

Treagus, S.H. and Sokoutis, D., 1992. Laboratory modelling of strain variation across rheological boundaries. J. Struct. Geol., 14: 405–424.

Turner, F.J. and Weiss, L.E., 1963. Structural Analysis of Metamorphic Tectonites. McGraw-Hill, New York, 545 pp.

Twiss, R.J., Protzman, G.M. and Hurst, S.D., 1991. Theory of slickenline patterns based on the velocity gradient tensor and microrotation. Tectonophysics, 186: 215–239.

Warner, M., 1990. Basalts, water, or shear zones in the lower continental crust? Tectonophysics, 173: 163–174.

Weijermars, R., 1992. Progressive deformation in anisotropic rocks. J. Struct. Geol., 14: 723–742.

Weiss, L.E., 1980. Nucleation and growth of kink bands. Tectonophysics, 65: 1–38.

White, S.H., Burrows, S.E., Carreras, J., Shaw, N.D. and Humphreys, F.J., 1980. On mylonites in ductile shear zones. J. Struct. Geol., 2: 175–187.

Williams, P.F. and Means, W.D., 1971. Rock folding: experiments on an artificial schist. Nature, 234: 90–91.

Williams, P.F. and Price, G.P., 1990. Origin of kinkbands and shearband cleavage in shear zones: an experimental study. J. Struct. Geol., 12: 145–164.

Yin, Z.M. and Ranalli, G., 1992. Critical stress difference, fault orientation and slip directions in anisotropic rocks under non-Andersonian stress systems. J. Struct. Geol., 14: 237–244.